

Reports

Optical Studies of Pulsar NP 0532

Abstract. *The period of optical pulsations from NP 0532 has been determined to within 3 nanoseconds on three different nights. The time rate of change of the period $(dP/dt)_p$ was 36.17×10^{-9} second per day. The pulse shape was highly asymmetrical with strong indications of structure. The ratio of the amplitude of the main pulse to that of the interpulse varied with time. No evidence was found for photon coincidences in the pulse on a time scale shorter than 2 microseconds.*

Since the discovery by Cocke *et al.* (1) of optical pulses from the pulsating radio source NP 0532 in the Crab Nebula, there have been several confirmations by other observatories (2, 3). We report here the results of some of our observations taken during the nights of 15, 16, and 21 February 1969 with the 61-cm reflecting telescope of the Mees Observatory. In this report we concentrate primarily on observations of the pulse period, the rates of change of the pulse period, and the mean pulse profile.

The equipment used was essentially the same as that developed for the observation of the pulsar CP 1919 (4). The method of data accumulation and

sorting is indicated in Fig. 1. A cooled 1P21 phototube generates pulses upon detecting photons collected by the telescope through a diaphragm 11 arc sec in diameter. These pulses are amplified, discriminated against noise, and then fed into one of 400 memory channels of a multiscaler. The choice of which memory channel is determined by a local clock which matches closely the period of the optical bursts. The master clock used was a frequency synthesizer (Monsanto Electronics) (5) which can be set to generate any signal from 0.01 hz to 1.3 mhz in 0.01-hz steps. The instrument was calibrated against both a cesium clock and the W.W.V. radio transmissions from Colorado about a

month prior to the observations. The frequency of the master oscillator was found to be correct to within 1 part in 10^8 and stable to 1 part in 10^9 per day. On each night this frequency synthesizer was set at a frequency 4×10^4 times as large as that expected for the pulsar NP 0532 after correction for orbital and diurnal Doppler effects. This frequency was then divided by a factor of 100 to a frequency ν_1 and by a further factor of 400 to give a frequency ν_0 . Pulses at frequency ν_1 were used to advance the memory address of the multiscaler, whereas pulses at frequency ν_0 reset the address to zero. In this way each count from the 1P21 is sorted into 400 channels representing its phase of arrival relative to pulse at the frequency ν_0 . The near equality of the frequency ν_0 and the pulsar frequency ensures that any repetitive signal from NP 0532 will be pulled out of the noise after a few minutes of integration.

The observed period of the pulsar is given by

$$P_{\text{obs}} = P_0 + (dP/dt)_p t + (\Delta P)_{\text{geo}} + A \sin \theta \quad (1)$$

where P_0 is the heliocentric period at time $t = 0$, $(dP/dt)_p$ is the average rate of change of that period since $t = 0$, and the third and fourth terms are corrections because of the earth's orbital and diurnal motions, respectively. In the final term, θ is the hour angle and the amplitude A depends on the coordinates of both the star and observer. In general, the variation of the observed period due to the above effects causes

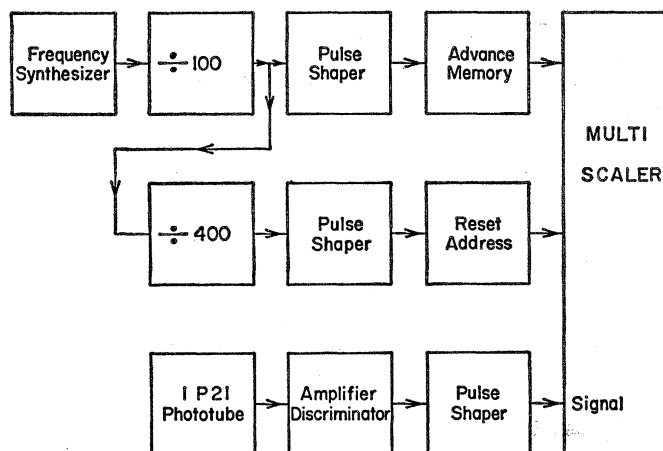
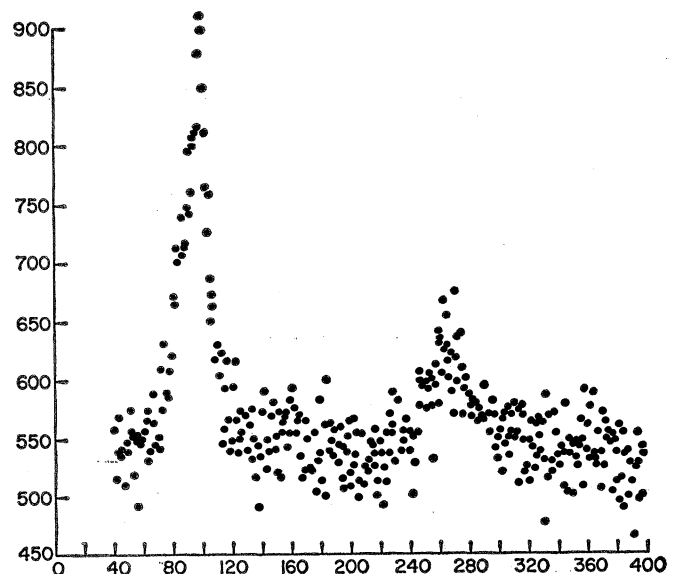


Fig. 1 (above). Schematic diagram of experimental equipment.

Fig. 2 (right). Optical pulse shape of NP 0532. The ordinate shows the number of counts and the abscissa is the channel number, each channel being 0.082 msec wide.



a shift in phase which shows up as a drift in the channel number of the pulsar peak during a night's observations. An additional drift is observed if the clock period, $P_{cl} = 1/\mu_0$, does not equal the geocentric period

$$P_g = P_0 + \Delta P_{geo}$$

The accumulated phase shift, in fractions of a pulsar period, is given by

$$\Delta\phi = \frac{1}{2P_g^2} \left(\frac{dP}{dt} \right) (\Delta t)^2 + \frac{nA}{2\pi P_g} \Delta (\cos \theta) + \frac{P_g - P_{cl}}{P_{cl}^2} (\Delta t) \quad (2)$$

where (dP/dt) includes the change in geocentric correction as well as $(dP/dt)_p$, n is the number of pulsar periods per day, and $\Delta (\cos \theta)$ is the difference in $\cos \theta$ since the start of the observations. The actual shift in the peak channel is $400 \Delta\phi$. Over a period of 2 or 3 hours, the first term is negligible. The difference, $P_g - P_{cl}$, may thus be found by subtracting the drift due to the diurnal term from $\Delta\phi$. The P_g thus found refers to the mean time of the observations, and the heliocentric correction we use to find P_0 also is that found at the mean time. The clock and geocentric and heliocentric pulsar periods for each night are given in Table 1. The estimated error in the heliocentric period for each night is 3×10^{-9} second. From the 6-day base line of our optical data, the periods (Table 1) give a value of $(dP/dt)_p$ of 37.7 ± 0.5 nsec/day. We have also fitted a second-order equation to the data in Table 1, together with a value of $P_0 = 0.033093188 \pm 4$ second determined from radio observations on 11 January 1969 (6). The linear term gives $(dP/dt)_p$ equal to 36.17 ± 0.07 nsec/day, whereas the quadratic term gives a value of 0.04 ± 0.04 nsec/day² for $(d^2P/dt^2)_p$. This latter figure is in our noise, and observations over at least a 100-day interval will be required in order for it to become significant. A good value of $(d^2P/dt^2)_p$ will allow us to test the theoretical model of NP 0532 developed by Gunn and Ostriker (7).

The fortuitous, approximate compensation between the second and third terms of Eq. 2 during our first night's observations has enabled us to obtain good profiles of the average pulse. Of the observations made during the night of 15 February 1969, three were obtained without any filters in the optical path. We have used these runs as an indication of the characteristic pulse

Table 1. Clock and pulsar periods as determined each night from the observed phase shift.

Date (U.T.)	Clock period (sec)	ΔP from phase shift (sec)	Geocentric pulsar P (sec)	Heliocentric pulsar P (sec)
February 16.1	0.033097500	-0.000000023	0.033097477	0.033094515
February 17.1	.033097571	-.000000039	.033097532	.033094546
February 22.1	.033097845	-.000000014	.033097831	.033094741

shape. The two runs with ultraviolet and blue filters on that night have been excluded from the analysis in case there is any systematic change of profile with color. On the other hand, most of the observations of 16 February 1969 were made during times when the value of $(d\phi/dt)$ was large enough to distort the pulse profiles significantly. The result of this distortion is to symmetrize the pulse shape somewhat. It is possible to compensate for this distortion by appropriate analysis, but again we have chosen not to use this data.

Although the phase slippage during each of the three runs of 15 February was small, we did observe predictable phase shifts between individual runs. Figure 2 shows a composite profile generated by superimposing these three runs after allowing for phase slippage. The composite curve does not reveal any feature not present on each of the individual profiles. The pulses are highly asymmetric with an average rise time, measured between the 10-percent and 90-percent level, of 1.75 msec. The fall time is 1.23 msec. About half the fall time, however, occurs between the 30- and 10-percent level. The half-width of the pulse is 1.49 msec. There is a suggestion of structure on the rising edge of the pulse—rapid rises followed by steps. This steplike structure, however, is barely at the level of statistical significance and deserves further observations. A well-defined feature, however, is the extremely sharp and narrow peak of the primary pulse, having a half-width of about 0.25 msec.

The pulse profiles that we obtained during the night of 16 February were similar to those published by Lynds *et al.* (3) and Cocke *et al.* (1). All these profiles are significantly different from the pulse shape in Fig. 2 which was obtained with a good match between clock and pulsar periods. We believe that this difference is due to a mismatch between apparent pulsar period and the reference clock. As previously noted, this will tend to make the profile appear more symmetrical.

Figure 2 also shows our observations of the profile of the interpulse. This pulse is significantly smaller and broader than the main pulse. It trails the onset of the primary pulse by about 14 msec and has a half-width of about 2.5 msec. These values are somewhat crude as a result of the relatively low counting rate in the interpulse.

Furthermore, we confirm the statement by Cocke *et al.* (1) that there appear to be gross changes in the relative amplitudes of the primary and secondary pulse. The ratio of the amplitude of the major pulse to that of the interpulse varies from about 2.3 to 3.8 over a period of roughly 3 hours.

We have also performed an analysis of the distribution of pulse heights coming directly from a preamplifier connected to the output of the 1P21 photomultiplier tube. The resolution time of this system is 2 μ sec. In this analysis we find no significant differences between the distributions of the following two classes of observations: (i) pulses taken randomly in time from the sky, and (ii) pulses accepted only during a 4-msec window centered on the main pulse from NP 0532.

Thus, we conclude that in a circle 11 arc sec in diameter centered on NP 0532 there is no evidence of bursts of optical photons separated in time by less than 2 μ sec. Porter (8) claims to have observed photon coincidences near NP 0532 on a 3-nsec scale. His system, however, covers a much larger area of the sky, and he may indeed be observing Cerenkov light from extensive air showers generated by gamma rays having energies of 10^{13} ev from NP 0532.

J. G. DUTHIE, C. STURCH
H. B. RICHER, P. RODNEY
*C. E. Kenneth Mees Observatory,
University of Rochester,
Rochester, New York 14627*

References and Notes

1. W. J. Cocke, M. J. Disney, D. J. Taylor, *Nature* **221**, 525 (1969).
2. R. E. Nather, B. Warner, M. Macfarlane, *ibid.*, p. 527.

3. R. Lynds, S. P. Maran, D. E. Trumbo, *Astrophys. J.* **155**, L121 (1969).
4. J. G. Duthie, C. Sturch, E. M. Hafner, *Science* **160**, 415 (1968).
5. Funds for the purchase of the frequency synthesizer were provided by the Eastman Kodak Company.
6. D. W. Richards and J. M. Comella, preprint of the Arecibo Ionospheric Observatory communicated by Y. Terzian.
7. J. E. Gunn and J. P. Ostriker, *Nature* **221**, 454 (1969).

8. N. A. Porter, *Int. Astron. Union Circ. No.* 2130 (1969).
9. We thank Dr. S. Sharpless for his constant encouragement and for making telescope time available, and to J. Geissinger for building electronic interfaces on very short notice. Supported in part by the Center for Naval Analyses of the University of Rochester. Such support does not imply endorsement of the content by the U.S. Navy.

3 March 1969

Planetary Probe: Origin of Atmosphere of Venus

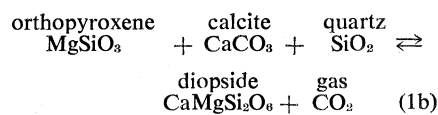
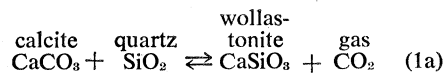
Abstract. *The high temperatures and chemical composition, as determined by space probe and terrestrial observation, suggest that the present atmosphere of Venus has formed by chemical interaction with the lithosphere. Although the precise reactions have not been identified, good theoretical approximations to the molecular abundance may be obtained from reactions applicable to terrestrial rocks. The high temperatures and chemical reactivity create conditions on Venus which are fundamentally different from those on the cooler terrestrial planets where the attainment of equilibrium is prevented by kinetic barriers.*

One model for the origin of the atmosphere of Venus is based on pervasive chemical reactions between gases in the basal atmosphere and minerals of the lithosphere (1, 2). This interaction model adequately accounts for the composition of the atmosphere if the unconfirmed high surface temperatures are accepted (3, 4). This report considers how this model fits the observational data obtained from recent planetary probes, in particular data from Venera 4.

Venera 4 descended into the atmosphere of Venus at a position within 10° of the equator and approximately 20° from the terminator on the dark side (5). The measurements, which were obtained at three atmospheric levels, indicate that the atmosphere of Venus is characterized by high temperatures and an abundance of CO₂. The data are also in essential agreement with the more indirect measurements of the Mariner V probe, which executed a simultaneous flyby of the planet (6). The only discrepancy involves the altitudes of the probes as compared with the planetary radius deduced from radar measurements made on Earth. Thus far no satisfactory explanation has been offered for this discrepancy, but the Mariner V data would lead to somewhat higher temperatures and pressures than those recorded by Venera 4 (7).

The high CO₂ pressure (20 atm or greater) must be explained by any comprehensive model of the planet. Urey (8) suggested that the CO₂ pressures in the atmospheres of the terrestrial plan-

ets might be governed by reactions of the following types



Reaction 1a was proposed to account for the CO₂ content of Earth's atmosphere, and 1b is applicable to certain terrestrial metamorphic terrains (9).

Urey explained the high CO₂ content in the atmosphere of Venus by proposing that kinetic barriers prevent equilibrium reactions such as 1a from shifting to the left; he believed that these kinetic barriers developed as a result of the

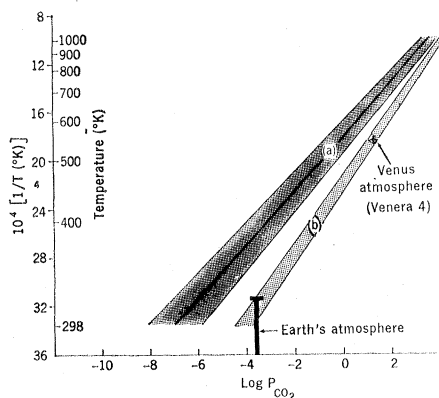


Fig. 1. Comparison of observational data for CO₂ abundance in the atmosphere of Venus and Earth with several reactions (1a and 1b) based on thermochemical data. The Venera 4 observational point corresponds to $T = 543^\circ\text{K}$ and a CO₂ pressure of 20 atm, whereas the bandwidths indicate uncertainties in the thermochemical data.

dry conditions on the planet. Thus the CO₂ concentration might build up far above the equilibrium value. However, at the high temperatures now accepted for the lower atmosphere and surface of Venus, these reactions should not only equilibrate but should also yield CO₂ pressures very close to those observed (1, 2). Actually equilibrium is required only on a geologic time scale; however, direct experiment (10) indicates that equilibrium is approached even on a laboratory time scale (~500 hours) at temperatures as low as 850°K.

If it is assumed that all the solid phases are of constant composition, the equation of equilibrium for reactions 1a and 1b may be written as

$$K_{1a} = P_{\text{CO}_2} \quad (2a)$$

$$K_{1b} = P_{\text{CO}_2} \quad (2b)$$

where P represents the fugacity of CO₂. At the surface temperatures and pressures which exist on Venus, these fugacities correspond essentially to partial pressures and are equal to the total pressure (11).

From thermochemical data (12), we may obtain K_{1a} and consequently P_{CO_2} as a function of the temperature (curve *a*, Fig. 1). The hatched bandwidth of this curve corresponds to the maximum and minimum values of the enthalpy and entropy contributions at 298°K and gives an indication of the uncertainty in the thermochemical data. The analogous data for K_{1b} , for reaction 1b has a somewhat different meaning. The low-pressure limit of the hatched area (curve *b*, Fig. 1) was determined in the same way, but the high-pressure limit was determined by considering the geologic conditions of the occurrence of the mineral assemblage under terrestrial conditions (9). The values of P_{CO_2} for both reactions 1a and 1b will also be influenced by deviations from stoichiometry of the solid phases, with probably the greatest effect on reaction 1b. An estimate of this effect, which takes into account the presence of such components as FeSiO₃ and CaFeSi₂O₆, shows that the curve *b* will be shifted toward lower pressures by a maximum of only a factor of 2 (9).

Also shown in Fig. 1 is the value of P_{CO_2} for Earth's atmosphere (8). Although the vertical height of the bar in this case includes the range of surface temperatures, coincidence with curve *b* may be fortuitous. However, Urey (8) believed that the value represents an ap-